Journal of Cleaner Production 327 (2021) 129489

Contents lists available at ScienceDirect

Journal of Cleaner Production

journal homepage: www.elsevier.com/locate/jclepro

Dry processing technology of exhaust gas emitted by roasting of rare earth concentrates with concentrated sulfuric acid

Jing Zhao [a,b], Bo Li [a,*], Xiaolin Wei [a,c]

[a] State Key Laboratory of High-Temperature Gas Kinetics, Institute of Mechanics, Chinese Academy of Sciences, Beijing, 100190, China
[b] Institute of Engineering Thermophysics, Chinese Academy of Sciences, Beijing, 100190, China
[c] School of Engineering Science, University of Chinese Academy of Sciences, Beijing, 100049, China

ARTICLE INFO

Handling Editor: Kathleen Aviso

Keywords:
Rare earth concentrates
Concentrated sulfuric acid roasting
Roasting exhaust gas
Wet spraying
Dry processing technology

ABSTRACT

At present, wet spraying is the main process for treatment of exhaust gas emitted by the concentrated sulfuric acid roasting method for decomposition of rare earth concentrates, which not only consumes a large amount of resources but also wastes the residual heat corresponding to temperatures of approximately 300 °C. In this paper, an exhaust gas dry processing technology that is completely different from the original wet spray process is proposed and successfully implemented in a rare earth roasting kiln. The dry process has successfully realized dust removal, cooling and acid condensation from exhaust gas through a cyclone separator and heat exchange-condensing acid system, and the waste heat can be converted into steam through a steam drum, which greatly simplifies the process for treatment of roasting exhaust gas. Compared with wet spraying, the dry process has the advantages of operational simplicity, small footprint, low energy consumption, low maintenance cost and no wastewater production, which makes it a promising process for the treatment of exhaust gas from rare earth roasting.

1. Introduction

The rare earth industry is known as "industrial monosodium glutamate" in modern industry, and rare earth resources have been listed as national strategic resources by many countries (Jordens et al., 2013). China is rich in rare earth resources and accounts for more than 70% of total global production (Chen et al., 2018). As the country pays more attention to environmental protection (Zhou et al., 2021), comprehensive utilization of resources (Yang et al., 2019) and treatment of pollutants (Zhong et al., 2017) will be the main problems and will restrict the survival and development of the rare earth production industry in the future. Among the steps in the process, the roasting of rare earth concentrates is the most energy consuming and the most polluting step in the whole process of rare earth production (Zheng et al., 2017). Therefore, there is an urgent need for a process of roasting rare earth concentrates that conserves resources and uses environmentally friendly technology.

At present, the main procedure for processing rare earth concentrates is high-temperature roasting with concentrated sulfuric acid, which has been widely used in recent decades (Huang et al., 2015). The main process involves mixing rare earth concentrates with a certain proportion of concentrated sulfuric acid to make a slurry (the weight ratio is 1.1–1.5) (Demol et al., 2019). Then, the slurry is sent to an internally heated rotary kiln to effect decomposition at 600–800 °C ((Demol et al., 2018). Although this technology has led to certain economic benefits, it produces large amounts of sulfur, fluorine, strong acid waste gas (Wang et al., 2010) and waste residue leached from water during high-temperature roasting of the concentrates (Wang et al., 2017). As shown in Fig. 1, The exhaust gas is mainly cooled by a multistage circulating spray tower (Wang et al., 2018), while the circulating cooling acid liquid continuously absorbs gaseous acid from the flue gas to generate a higher concentration of mixed acid (Bian et al., 2018). Then, the mixed acid is separated with acid distillation equipment to realize the recovery and reuse of sulfuric acid and fluoric acid (Li et al., 2021). However, the process system is very complex, natural gas consumption is large, and the energy and resource losses are serious, as reflected in the following aspects:

- **Unutilized waste heat from exhaust gas:** a large amount of cold water needs to be sprayed into the sediment pool and spray tower to effect cooling of the exhaust gas. The temperature of the high-temperature exhaust gas at the end of the kiln is decreased from

* Corresponding author.
E-mail address: libo@imech.ac.cn (B. Li).

https://doi.org/10.1016/j.jclepro.2021.129489
Received 16 July 2021; Received in revised form 20 October 2021; Accepted 23 October 2021
Available online 26 October 2021

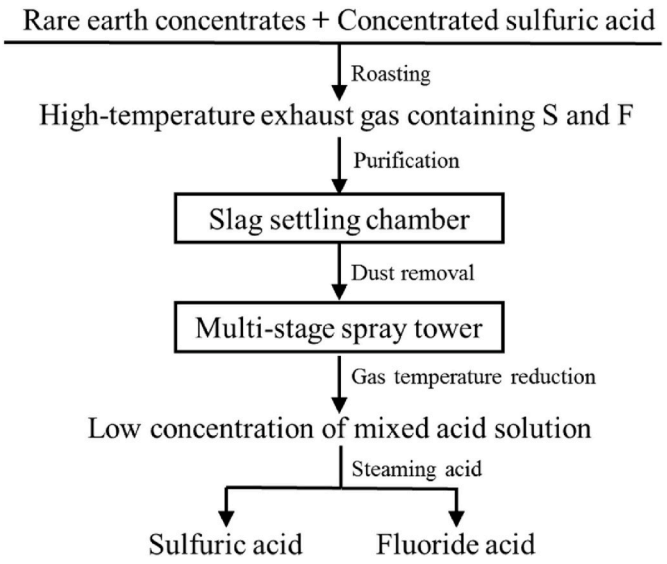

Fig. 1. Schematic of common purification process for exhaust gas emitted by roasting of rare earth concentrates with concentrated sulfuric acid.

300 to approximately 60 °C along with sediment and water washing (Li et al., 2021). In this process, all the perceivable and latent heat of the exhaust gas is absorbed by the cooling water and finally released into the atmosphere, which causes thermal waste.

- **High energy consumption in the acid steaming process:** the mixed acid solution is produced after the cooling water in the spray tower contacts the flue gas. This part of the mixed acid liquid needs to be repeatedly used as a spray to reduce water consumption and increase the concentration of the mixed acid (Zhao et al., 2013). In the process, it needs to exchange heat with the cooling water and continue to cool. The final mixed acid is distilled and separated through equipment such as a graphite evaporator and condenser. The heat source steam in this process is generated by combustion in the natural gas boiler, and the use of steam naturally causes consumption of large amounts of natural gas and a loss of demineralized water.
- **High costs of equipment repair and maintenance:** the circulation of the mixed acid solution in the spray tower requires a large amount of cooling water to effect cooling. However, the efficiency of heat exchange is relatively low due to the small temperature difference. Therefore, to achieve cooling of the mixed acid, a large number of graphite heat exchangers are needed, which significantly increases the investment in equipment. Production is even reduced in the summer due to poor cooling. In addition, the extensive use of circulating cooling water also brings evaporation and wind loss of water resources. At the same time, the heat exchanger is prone to blockage and damage, and the investment in equipment maintenance and replacement is also large.

Therefore, it is urgently necessary to research and develop a new energy-saving and environmentally benign process for treatment of roasting flue gas and equipment to simplify the process for treatment of flue gas and mixed acid, increase the concentration of acid, and improve the efficiency of kiln systems. However, most studies have focused primarily on the roasting process (Li et al., 2019), thermal decomposition (Nie et al., 2018) and recovery and separation (Swain and Mishra, 2019) of rare earths and have failed to address the treatment of exhaust gas. In view of the various disadvantages of the wet spray treatment, our groups designed and built a set of dry treatment processes for roasting exhaust gas. In this paper, we first introduce the main process and equipment for dry processing of exhaust-gas from rare earth concentrates made by roasting with concentrated sulfuric acid. Second, the key operating parameters (condensate acid, steam, fluorine emission, etc.) of the process are discussed and analyzed for actual production of the roasting kiln. Finally, the effectiveness and practicality of exhaust-gas dry processing are evaluated and compared with those of the original wet spray. The method and data from this study will be valuable for the development of new strategies to treat roasting exhaust gas.

2. Experiment section

2.1. Exhaust gas source

As illustrated in Fig. 2, exhaust-gas dry processing as industrial demonstration plant has been successfully carried out in an actual roasting kiln in production, located in Baotou, Inner Mongolia Autonomous Region, China, which handles 1.5 tons/h of rare earth concentrates (Bayan obo ore) and produces approximately 10,015 Nm^3/h of exhaust gas. The roasting kiln utilizes an internal heating method, the heat source comes from the combustion of natural gas, and the consumption is 225 Nm^3/h, which keeps the temperature of the kiln head at 600–800 °C. The chemical principle of concentrated sulfuric acid roasting is to convert water-insoluble $REFCO_3$ and $REPO_4$ into water-soluble $RE_2(SO_4)_3$ (Xie et al., 2014). The ratio of rare earth concentrates to concentrated sulfuric acid is 1:1.26. At the same time, to convert the byproduct pyrophosphoric acid into a precipitate, the roasting process still needs to accommodate the addition of approximately 9% (weight fraction) iron ore concentrate (with Fe content not less than 60%) to mix with rare earth concentrate (Chen et al., 2012). Because the solubility of the generated rare earth sulfate is very low (Kim and Osseo-Asare, 2012), the amount of water consumed must be approximately 30 times that of the rare earth concentrate. After the rare earth sulfate water leaching solution is pretreated by adding magnesium oxide and other chemical substances, iron, thorium, phosphorus, aluminum, zinc, and manganese are removed, and the pure rare earth sulfate solution can be obtained by filtration (Chen et al., 2020).

The chemical composition of rare earth concentrates is shown in Table 1, and the total rare earth oxides (TREO) determine the quality of concentrates. The acidic exhaust gas produced by roasting with concentrated sulfuric acid mainly comes from volatilization of concentrated sulfuric acid at high temperature and the following chemical reactions R1-R8 (Wang et al., 2010) and R9-R12 (Zhao et al., 2013):

$$2REFCO_3 + 3H_2SO_4 = RE_2(SO_4)_3 + 3H_2O\uparrow + 2CO_2\uparrow + 2HF\uparrow \quad (R1)$$

$$2REPO_4 + 3H_2SO_4 = 2RE_2(SO_4)_3 + 2H_3PO_4 \quad (R2)$$

$$Th_3(PO_4)_4 + 6H_2SO_4 = 3Th(SO_4)_2 + 4H_3PO_4 \quad (R3)$$

$$Fe_2O_3 + 3H_2SO_4 = Fe_2(SO_4)_3 + 3H_2O\uparrow \quad (R4)$$

$$CaF_2 + H_2SO_4 = CaSO_4 + 2HF\uparrow \quad (R5)$$

$$4HF + SiO_2 = SiF_4\uparrow + 2H_2O\uparrow \quad (R6)$$

$$2H_3PO_4 = H_4P_2O_7 + H_2O\uparrow \quad (R7)$$

$$H_4P_2O_7 + Th(SO_4)_2 = ThP_2O_7 + 2H_2SO_4 \quad (R8)$$

$$H_2SO_4 = SO_3\uparrow + H_2O\uparrow \quad (R9)$$

$$2SO_3 = 2SO_2\uparrow + O_2\uparrow \quad (R10)$$

$$H_4P_2O_7 + 2CaSO_4 = Ca_2P_2O_7 + 2H_2SO_4 \quad (R11)$$

$$2Fe_2(SO_4)_3 + 3H_4P_2O_7 = Fe_4(P_2O_7)_3 + 6H_2SO_4 \quad (R12)$$

The main components and contents of the roasting exhaust gas, as determined by gas detection, are shown in Table 2. Among them, the main components (H_2O, CO_2, O_2 and N_2) are mainly formed by natural gas combustion; sulfuric acid mist (H_2SO_4) mainly comes from the volatilization of roasting sulfuric acid; fluorides (HF and SiF_4) are mainly formed through reactions R1 and R5-R6; and the source of SO_3

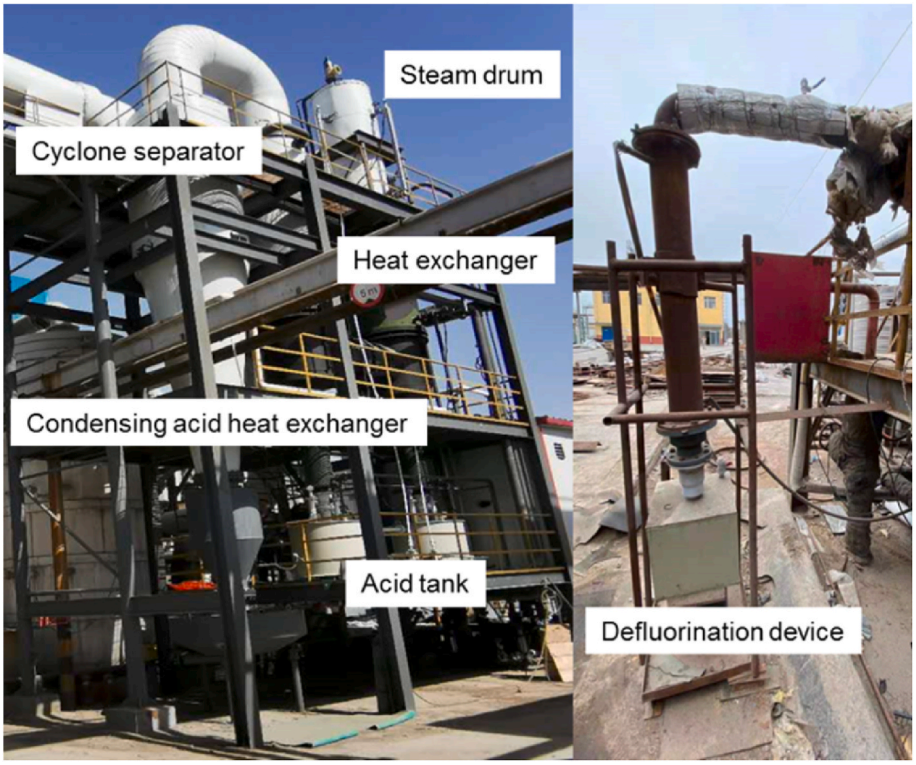

Fig. 2. Picture of real products for exhaust gas treatment by dry processing technology.

Table 1
Chemical composition and content of rare earth concentrates (wt.%).

Quality	Non-rare earth impurity content									
TREO	S	F	Ba	Th	Fe	Si	Ca	Mg	P	Moisture
55 ±5	2.33 ±0.2	8.68 ±0.9	0.9 ±0.1	0.062 ±0.01	3.24 ±0.3	0.88 ±0.1	9.39 ±0.9	0.22 ±0.2	3.4 ±0.3	13 ±3

Table 2
Composition and volume flow rate of the exhaust gas.

Main compositions	H_2O	CO_2	O_2	N_2	Total volume flow rate: 10,015 Nm^3/h
Flow rate (Nm^3/h)	1503.6	338.8	1313.9	6671.4	
Acid compositions	Fluoride	H_2SO_4	SO_2	SO_3	
Flow rate (Nm^3/h)	21.6	107.5	23.2	35.0	

and SO_2 is the high-temperature decomposition of sulfuric acid in reactions R9 and R10 and the oxidation of sulfur bearing ores.

2.2. Process description

The roasting process used in rare earth plants usually produces high-temperature acid-containing waste gas at approximately 300 °C. As shown at the top of Fig. 3, most rare earth manufacturers currently use a slag settling chamber to remove dust, use the quench and mixed cooling tower to cool, and then connect the two-stage PVC spray tower to spray and wash the exhaust gas to remove most of the fluoride, sulfuric acid mist and remaining dust. The main adsorption reactions (R13-R16) are:

$$H_2SO_4\ (mist) + H_2O = H_2SO_4\ (liquid) \quad (R13)$$

$$SO_3 + H_2O = H_2SO_4 \quad (R14)$$

$$HF + H_2O = HF{\bullet}H_2O \quad (R15)$$

$$SiF_4 + 2HF = H_2SiF_6 \quad (R16)$$

The residual exhaust gas is mostly composed of noncondensable gases such as N_2, CO_2, and SO_2, and the exhaust gas can be directly discharged through the chimney after desulfurization. The mixed acid from the spray tower is separated by steam heating, and then the fluorosilicic acid and sulfuric acid are recycled and reused after condensation of the circulating cooling water. However, the spraying process not only requires a large amount of cooling water but also the concentration of the recovered waste acid is also relatively low and requires further concentration and separation through the evaporator and condenser. In this process, a large amount of heat carried by the high-temperature flue gas is not effectively utilized. The process also has many problems, such as high energy consumption, complex processes, long processing times and wasted water resources.

Compared with the original wet processing, the dry processing technology introduced in this paper greatly simplifies the treatment of exhaust gas by realizing recovery of residual heat (see the bottom of Fig. 3). With a four-way pipe and blind plate, the kiln tail exhaust gas can be switched freely between new dry processing and original wet spray without any impact on the original process, and this ensures that the exhaust gas is switched back to the original system in an emergency. According to the results measured by the pitot tube, approximately half of the exhaust gas is shunted to enter the dry processing system during

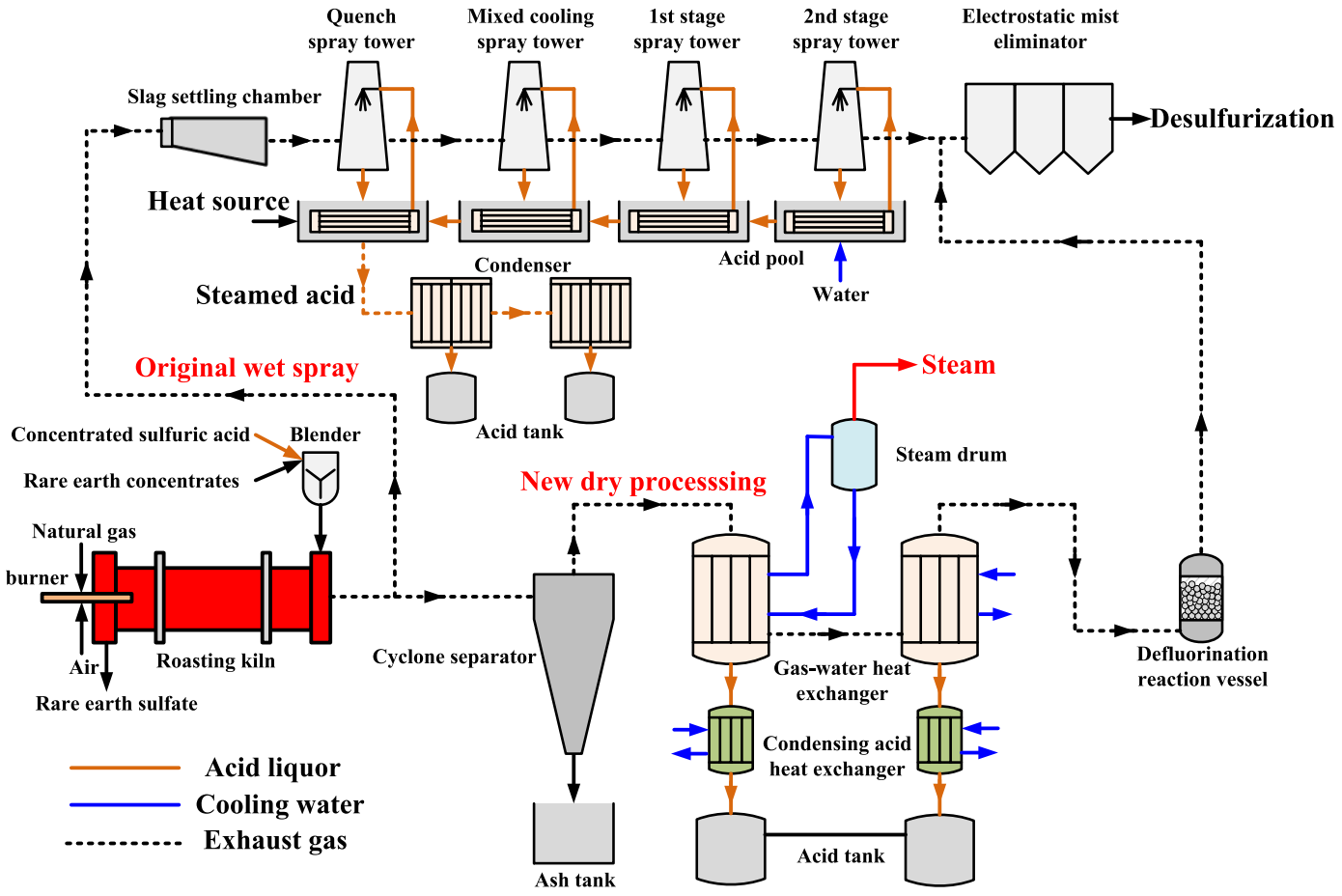

Fig. 3. Schematic diagram of the new dry process (bottom) and original wet spray (top).

the trial. First, the exhaust gas is driven to the cyclone separator through a bypass in front of the slag settling chamber of the original system for dust removal. In this process, more than 85% of the dust is removed, which prevents the blockage of the heat-exchange equipment and decreases heat transfer efficiency caused by dust deposition. Second, the exhaust gas is cooled through two sets of graphite heat exchangers. In the 1st heat exchanger (the heat transfer area is 203 m^2), the temperature of the exhaust gas is reduced from 300 °C to 170 °C by circulating hot water from the steam pocket, and the flow rate of the pump is 100 m^3/h. Waste heat is continuously used to convert hot water into saturated steam (approximately 130 °C). At this time, the sulfuric acid in the exhaust gas precipitates out in large quantities with decreasing temperature and enters the concentrated sulfuric acid storage tank after further cooling by the condensate acid cooler (the rate for circulating cooling water is 20 m^3/h). In the 2nd heat exchanger (the heat transfer area is 179.8 m^2), the temperature of the exhaust gas is further decreased from 180 °C to approximately 50 °C by circulating cooling water, and the flow rate of the pump is 40 m^3/h. In this process, residual sulfuric acid, hydrofluoric acid, and fluosilicic acid further precipitate from the exhaust gas and enter the mixed acid storage tank after cooling by the condensate acid cooler. To further remove the residual fluoride in the exhaust gas and decrease the effect of fluoride on the desulfurization process (organic amine method), the exhaust gas is introduced into a reaction vessel containing a regenerative adsorbent used to achieve the removal of residual fluoride (HF or SiF_4).

2.3. Key equipment

The key equipment for the dry process includes a cyclone separator, heat exchange-condensing acid system and dry defluorination device. The details are described as follows:

(1) Cyclone separator

As the first treatment process for high-temperature exhaust gas, the cyclone separator carries out the removal of coarse dust and initially removes a large amount of dust in the exhaust gas to reduce the damage to the equipment caused by dust friction. The working principle is that the roasting exhaust gas impacts the baffle at a rate of 13–18 m/s, which causes the gas flow to change sharply, and then the inertial force of the dust itself is used to separate it from the exhaust gas (Noh et al., 2018); this achieves a dust removal efficiency of more than 85%.

(2) Heat exchange-condensing acid system

After dust removal, the exhaust gas is introduced into the second process (waste heat recovery system), which mainly uses a graphite heat exchangers and a steam drum, which are the core devices of dry processing technology. The device uses gas-water heat exchange, which decreases the gas temperature from 300 °C to 50 °C through two-stage heat exchange. Heated circulating hot water generates steam in the steam drum through flash evaporation technology. To inhibit corrosion of the equipment, the exhaust gas is required to flow through the tube side of the heat exchanger and the water is required to go through the shell side. When the flue gas is cooled by the waste heat boiler, the acid gas also releases latent heat and condenses into a liquid, which is collected by the acid recovery system for recycling. According to the difference in the condensation temperature, sulfuric acid and fluoric acid can be separated to realize the separate recovery of high-concentration sulfuric acid and hydrofluoric acid.

(3) Dry defluorination device

The dry defluorination process is mainly realized by renewable or recyclable adsorbents. Therefore, the defluorinated adsorbent must not only be able to achieve high-efficiency purification of fluorine-containing tail gas, but also not produce secondary pollutants. At the same time, it also needs to realize recycling to ensure that can achieve optimal defluorization effect with maximum reduction in business operating costs. After many experimental analyses, a defluorinated adsorbent with a fluoride salt as its main component was selected. The adsorbent has good selective absorption of fluoride. This adsorption is not a general physical adsorption but is based on the chemical action of fluoride salts on fluoride. The adsorbent forms a chemical complex with fluoride that can be decomposed by heating, and this allows reuse of the adsorbent (Tavakoli et al., 2010).

In the preparation of the adsorbent, sodium silicate with a modulus between 3 and 3.3 is added, and the amount of addition is controlled at approximately 5%, which is conducive to shaping of the adsorbent. In addition, SiO_2 in sodium silicate reacts with HF in the actual absorption process to give SiF_4 (Wang et al., 2010); this process leads to formation of numerous pore channels in the adsorbent particles, thereby increasing the absorption specific surface area of the adsorbent. To further enhance the mechanical strength of the adsorbent, it is necessary to put the shaped adsorbents into an oven for drying at approximately 105 °C.

3. Results and discussion

3.1. Operation condition of key equipment

3.1.1. Evaluation of cyclone separator performance

During operation of the dry system, as illustrated in Fig. 4, the main acid oxides present as dust in the exhaust gas are P_2O_5 and SO_3, and the basic oxides include CaO, Fe_2O_3, La_2O_3, CeO_2 and Nd_2O_3. Therefore, the specific gravity of the dust is relatively large due to the presence of rare earth oxides. The figure also shows that ash particles with sizes larger than 10 μm account for approximately 70% of the total, and these large particles are easily removed by their own inertial force under the action of the cyclone separator. Other particles with smaller sizes can be removed partly by aggregation into larger particles and partly by adhering to larger particles.

To evaluate the performance of the cyclone separator, a laser dust analyzer using the principle of light scattering was employed to determine the concentrations of particulate matter (PM) in the exhaust gas at the inlet and outlet of the cyclone separator (Han et al., 2021). To prevent high-temperature exhaust gas from damaging the equipment, high-purity N_2 can be used to dilute and cool the measured exhaust gas before detection of the concentration. The results determined after conversion are shown in Table 3, and they indicate that the concentration of PM in the exhaust gas reached 3.11–3.25 g/Nm^3. If the dust was not removed from the exhaust gas, the heat exchanger would be blocked due to ash deposition, which would affect the safe and stable operation of the equipment. After the exhaust gas passed through the cyclone separator, the average concentration of PM in the exhaust gas was reduced to approximately 0.44 g/Nm^3, and the efficiency for removal of PM reached 86%, indicating that the equipment met the design requirements. Although some of the particles were still not removed, the residual particulate matter mainly consisted of fine particles with strong penetration. In the subsequent heat exchange and acid condensation process, they were carried out of the heat exchanger by the acid liquid and did not have a significant impact on the heat exchangers.

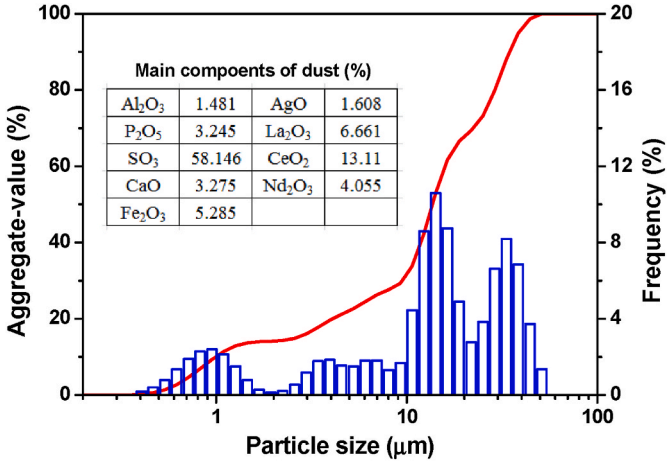

Fig. 4. Mass-based particle size distribution of dust in the exhaust gas.

3.1.2. Steam production with waste heat from the exhaust gas

In the steam production process, the detailed diagram of exhaust gas-water heat exchange is shown in Fig. 5. The exhaust gas enters from the top of 1st heat exchanger and flows out from the top of 2nd heat exchanger and the flow direction of cooling water is exactly opposite to that of exhaust gas. 1st heat exchanger is connected with the steam drum, and the soft water for steam production is filled from the bottom of the steam drum. When the system reaches stable operation, the liquid level of the steam drum basically remains unchanged, and at this time, it can be approximately considered that the water filling rate is equal to the steam producing rate. The circulating cooling water of 2nd heat exchanger comes from the water filling station, and the heat adsorbed by the cooling water can be discharged through cooling tower.

As illustrated in Fig. 6(a), the temperature change of the exhaust gas after passing through the dry process system was measured in real time with preinstalled thermometers, with data including inlet temperature, temperature between the 1st and 2nd heat exchangers, and outlet temperature. The temperature fluctuated within the normal range, and the operating conditions were relatively stable during controlled operation of the system. After passing through the 1st heat exchanger, the temperature of the exhaust gas was decreased to the designed 170 °C, and the gas temperature after passing through the 2nd heat exchanger was consistently controlled below 50 °C. Automatic operation of the system was realized with the programmable logic controller (PLC) automatic control system. As shown in Fig. 6(b), to ensure that the steam drum produces steam stably, it is necessary to keep the frequency of the hot water circulating pump (1st heat exchanger) constant. However, it is also necessary to adjust the flow of cooling water by constantly adjusting the frequency of the circulating cooling pump (2nd heat exchanger) to realize an exhaust gas outlet temperature of less than 50 °C.

Since the temperature of the exhaust gas emitted from the end of the roasting kiln decreased from 300 to 170 °C after passing through the 1st heat exchanger, the heat released was absorbed by the circulating hot water for production of steam by flash vaporization in the steam drum. The key temperature parameters of the steam drum during stable operation of the dry system are shown in Fig. 7. The figure shows that when the temperature in the steam drum reached approximately 135 °C, the circulating hot water continued to adsorb heat from the exhaust gas and was further heated to approximately 140 °C. The steam drum produces steam continuously and consistently when using a heat transfer temperature difference of approximately 5 °C. After testing, the waste

Table 3
Dust removal efficiency of the cyclone separator during dry system running.

Batch	Inlet concentration (g/Nm^3)	Outlet concentration (g/Nm^3)	Efficiency of cyclone separator (%)
1	3.16	0.52	83.54
2	3.11	0.38	87.78
3	3.25	0.43	86.77
Average	**3.17**	**0.44**	**86.12**

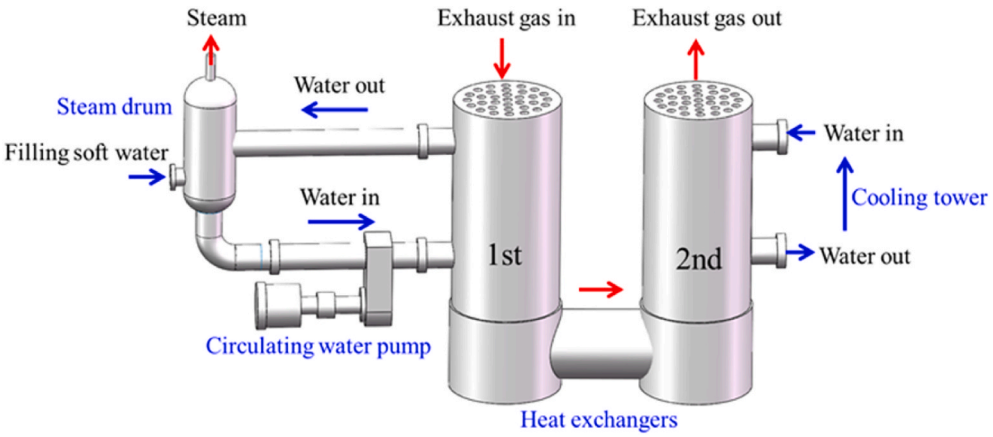

Fig. 5. Schematic of the gas-water heat exchanger portion in the dry processing system.

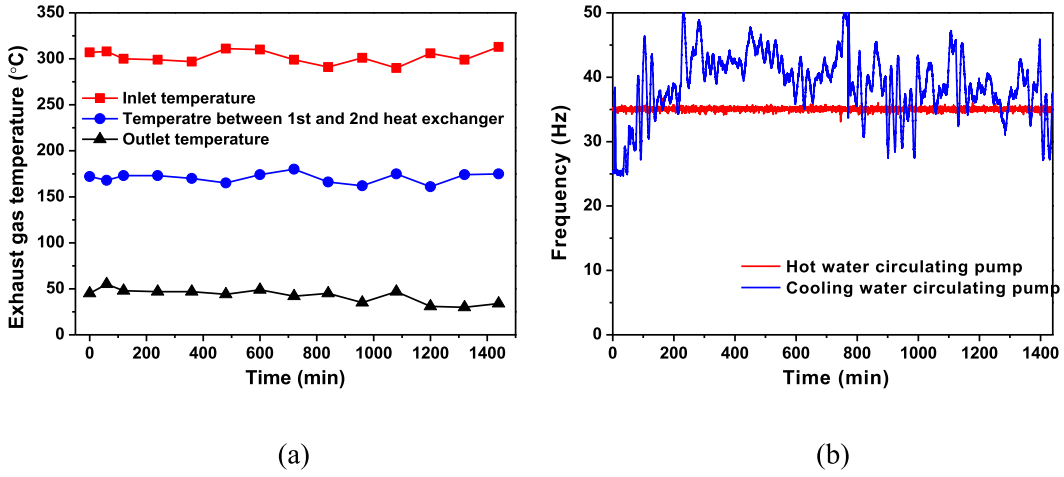

Fig. 6. (a) Temperature variation of exhaust gas after passing through the dry process system during a one day monitoring period; (b) frequency variation of the circulating water pump within one day.

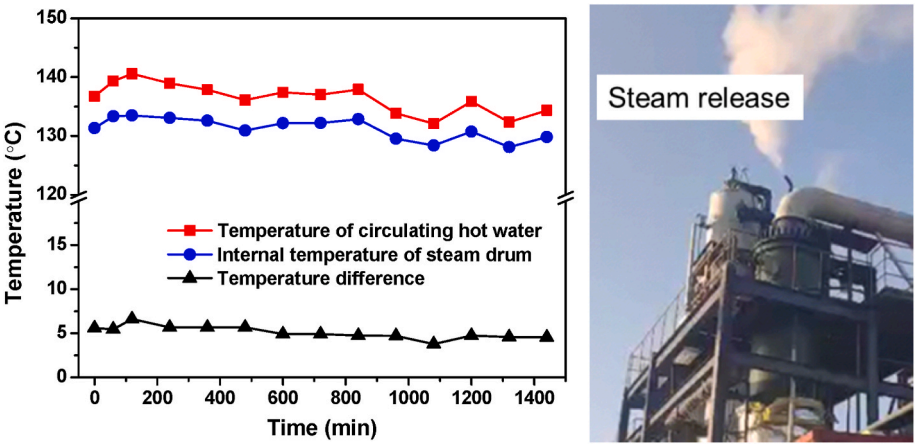

Fig. 7. Variations in key temperature parameters of the steam drum during regular production within one day.

heat from the high-temperature exhaust gas produced 0.64 tons/h of steam. When the system entered a stable operating state, the released heat of exhaust gas should be equal to the adsorbed heat by the circulating hot water and also equal to the latent heat of vaporization of steam produced. According to the calorie calculation formula, the required amount of soft water circulation can be calculated as about 65 t/h and the weight fraction loss in steam was about 1%. At the same time, the water used to produce steam needs to be soft water to prevent scaling. The temperature of steam production is usually controlled by the pressure of the steam pipe network. In this paper, the steam grid-connection pressure of the dry process system was approximately 0.32 MPa, so the temperature of steam production was approximately

135 °C.

3.2. Evaluation of the acid condensing process

3.2.1. Condensing acid amount and composition analysis

After the acidic substances in the exhaust gas are condensed in the dry process system, they are first stored in an acid condensing tank made of polypropylene (PP). When the acid liquid level reaches the set value, the acid pumps discharge the acid to the storage pool, and the acid is used for the roasting process. As shown in Fig. 8, a weight meter under the acid tank was used to determine the weight of the acid tank under the 1st heat exchanger; the weight periodically changed within the range 600–1050 kg, and the average amount of acid condensed within a 72 h period was approximately 133.3 kg/h. In the same way, the weight of the acid tank at the lower part of the 2nd heat exchanger varied periodically within the range 500–900 kg, and the average amount of acid condensed within a 72 h period was approximately 272.25 kg/h.

The acid concentration in the acid tank was measured by titration (Asakai et al., 2010), and the specific gravity of the acid was measured by a hydrometer. The results are shown in Table 4. According to these analyses, the acid in the tank below the 1st heat exchanger was mainly H_2SO_4 with an average concentration of 77.59%, which is much higher than the concentration of sulfuric acid obtained by the original wet spray system before the acid is distilled and can be used in the rare earth roasting process. The acidic liquid in the tank below the 2nd heat exchanger was mixed acid comprising sulfuric acid, hydrofluoric acid and fluorosilicic acid, but mainly H_2SO_4 with a concentration of 56.42%. After purification by distillation, the acid can be used in the rare earth roasting process. Using the previous acid condensation data and converting to 100% acidity, the calculation showed that the amount of sulfuric acid precipitated in the flue gas during the 72 h operation time was 257.03 kg/h (the total amount of sulfuric acid in the two tanks); the rate for precipitation of fluoric acid (HF and H_2SiF_6) was 21.01 kg/h. The recovery ratio of acid is defined as the ratio of the acid condensed to the total amount of acid in the dry system. During the test, the rate of exhaust gas flow into the dry process system was approximately 4529 Nm^3/h, constituting approximately half of the total flow of roasting kiln exhaust gas. According to the analysis of exhaust gas composition shown in Table 2, the main sources of condensed sulfuric acid were sulfuric acid mist (H_2SO_4) and sulfur trioxide (SO_3) in the exhaust gas, and the total amount (converted to 100% H_2SO_4) in the dry system was 281.93 kg/h. Fluoric acids (HF and H_2SiF_6) were mainly formed by the condensation of fluorides (HF and SiF_4) in the exhaust gas, and the total amount in the system was 22.49 kg/h. Therefore, the recovery ratios for sulfuric acid and fluoride were 91.17% and 93.44%, respectively.

3.2.2. Acid balance analysis for dry process system

The residual acidic components in the exhaust gas after the dry process were also measured before they entered the defluorination system. The results are shown in Table 5. A glass fiber filter cartridge was connected in series with an absorption bottle containing an isopropanol solution to collect the sulfuric acid content present in the exhaust gas after passing through the dry process system. The sampling filter cartridge captured small droplets of sulfuric acid; the sulfur trioxide gas and small droplets that penetrated the filter cartridge were captured with a series of isopropanol solutions. The content of sulfuric acid was measured by ion chromatography (IC) (Zhang et al., 2007). The sampling process was as follows: the sampling probe with the filter cartridge was placed deep into the sampling point in the pipe for continuous sampling over 30 min with constant velocity, and the heating temperature of the sampling probe was kept at 120–130 °C to prevent condensation of other substances from interfering with the experimental results. After sampling, the filter cartridge was carefully removed and placed into a screw-top wide-mouth polyethylene tube. To ensure the stability of the isopropanol absorption solution, measurements were completed within 4 h. The sampling process for fluoride was the same as that for sulfuric acid mist. A standard NaOH solution was used as the absorption liquid, and the content of F^- was determined with an ion-selective electrode (ISE).

As shown in the table, after passing through the dry system (for dust removal and cooling), the average flow rate detected for the exhaust gas decreased to approximately 3942 Nm^3/h due to condensation of sulfuric acid and fluoric acid. The average concentration of sulfuric acid mist (H_2SO_4) and sulfur trioxide (SO_3) was 3798 mg/Nm^3 and that of fluoride (HF and SiF_4) was 107.5 mg/Nm^3 in the residual exhaust gas. Thus, it can be calculated that the flow rates of residual sulfuric acid mist/SO_3 and fluoride in the exhaust gas were 14.98 and 0.42 kg/h, respectively. Assuming that the acid in the dry process system mainly consisted of condensing acid and residual acid in the exhaust gas, a detailed acid balance analysis can be performed for the dry system, and the results are shown in Fig. 9. The total amount of condensed acid and residual acid was slightly lower than the amount of acid entering the system (the error was within 5%), mainly because a small amount of acid may be carried away by dust during the cyclone dust removal process. These results confirm that the data for acid condensation and detection are accurate.

3.2.3. Comparison of recovered acid amount between dry process and wet spraying

If all of the exhaust gas (10,015 Nm^3/h) enters the dry process system, it produces approximately 378.92 kg of sulfuric acid and 30.98 kg of fluoric acid per ton of concentrate through the two-stage heat exchange systems used in the dry system process. According to the results

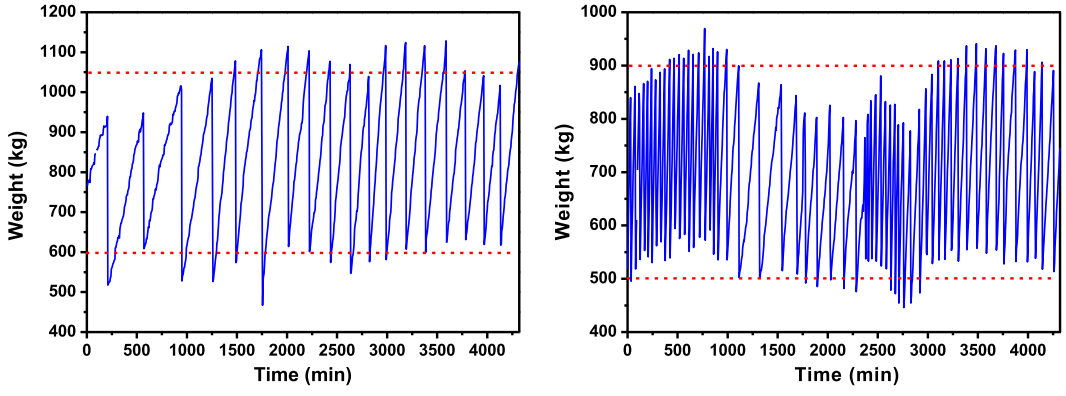

Fig. 8. Weight variation of acid tanks over 72 h: (a) acid tank under the primary heat exchanger; (b) acid tank under the second heat exchanger.

Table 4
Main compositions and concentrations in two acid tanks.

Batch	Acid tank (1st heat exchanger)				Acid tank (2nd heat exchanger)			
	specific gravity	H_2SO_4	HF	H_2SiF_6	specific gravity	H_2SO_4	HF	H_2SiF_6
	g/ml	%	%	%	g/ml	%	%	%
1	1.70	75.87	0.35	0.00	1.54	54.42	5.67	2.34
2	1.68	78.52	1.23	0.00	1.49	56.12	4.33	2.04
3	1.70	80.38	1.33	0.00	1.53	57.98	5.39	1.98
4	1.68	76.92	1.39	0.00	1.54	58.32	4.90	2.15
5	1.74	76.26	1.42	0.00	1.56	55.26	5.16	1.84
Average	**1.7**	**77.59**	**1.14**	**0.00**	**1.53**	**56.42**	**5.09**	**2.07**

Table 5
Content of residual acid substances in the exhaust gas after dry process system.

Batch	1	2	3	Average
$H_2SO_4 + SO_3$ (mg/Nm^3)	3980.0	3719.0	3695.0	**3798.0**
$HF + SiF_4$ (mg/Nm^3)	129.1	109.7	83.7	**107.5**
Flow rate (Nm^3/h)	4074	3792	3963	**3943**

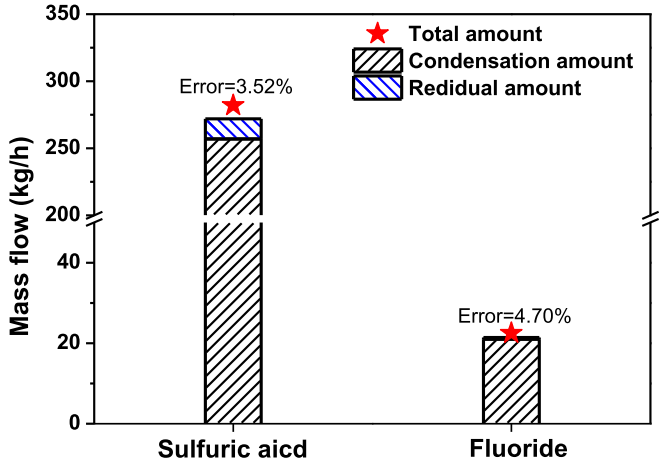

Fig. 9. Calculated results for acid balance in the dry process system.

shown in Table 4, the production of hydrofluoric acid (HF) and fluorosilicic acid (H_2SiF_6) were calculated as 22.02 kg and 8.96 kg per ton of concentrate based on their concentration ratio in the mixed acid. In 2020, according to production statistics provided by the plant, the average yield of sulfuric acid was 393 kg and that of hydrofluoric acid was 23 kg per ton of concentrate with the original wet spray system. As illustrated in Fig. 10, the yields of H_2SO_4 and HF in the current dry process were basically consistent with those of the original wet spray system. However, the dry process greatly simplifies the system used for treatment of the exhaust gas from rare earth roasting kilns, eliminates complicated processes such as spray and acid steaming, and produces steam. The dry process produced pure sulfuric acid with a concentration of approximately 77.6%, which can be directly used in roasting systems, while the wet spray process only produced mixed acid with a concentration of 36% and the concentration of sulfuric acid must be increased to greater than 65% through the steaming process before it can be used. In addition, residual sulfuric acid mist and fluoride can be further recovered by a mist eliminator and defluorination system. Therefore, the dry process has obvious advantages and significant economic benefits compared with the original wet spray process.

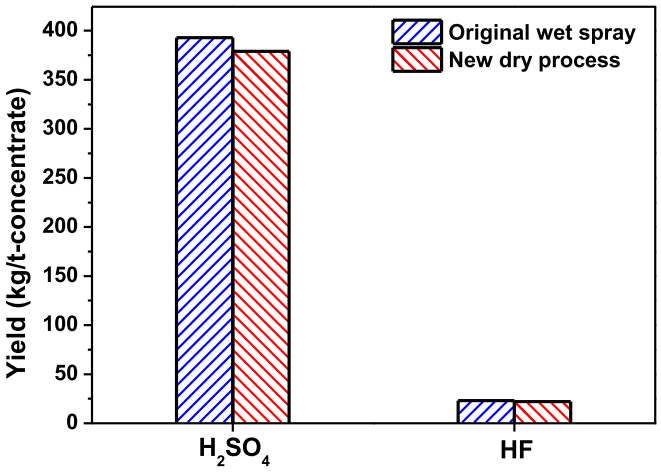

Fig. 10. Comparison of the yields of H_2SO_4 and HF per ton of concentrate for the dry process and the original wet spray process.

3.3. Dry defluorination process

3.3.1. Fluoride adsorption

According to the results in Section 3.2.2, although 93% of the fluoride (HF and SiF_4) was removed by acid condensation in the dry process system, the concentration of residual fluoride in the exhaust gas (above 100 mg/Nm^3) was still too high for the desulfurization process (less than 30 mg/Nm^3). To avoid the influence of fluoride on the desulfurization process, it is necessary to further remove fluoride and realize resource recovery. In this work, the removal of fluoride in flue gas is realized by using the selective absorption of fluoride by villiaumite. Adsorption and recovery of HF and SiF_4 can be realized at 20–80 °C through the R17 (Gromov, 2014) and R18 (Singh and Moharil, 2020), respectively.

$$MeF_m + nHF = MeF_m{\cdot}nHF \quad \text{(R17)}$$

$$xMeF_m + SiF_4 = x(MeF_m){\cdot}SiF_4 \quad \text{(R18)}$$

where Me denotes alkali and alkaline earth metals (such as Na, K, Ca and Ba, etc.), m denotes molecular stoichiometry, and x and n indicate molar ratios.

Fig. 11 illustrates that the regeneration process of adsorbents mainly generated sodium fluoride (NaF) by heating. When the adsorbents were heated above 160 °C, the generated sodium bifluoride ($NaHF_2$) decomposes to form NaF and HF. As the heating temperature further is increased above 600 °C, the generated sodium fluorosilicate (Na_2SiF_6) is decomposed to form NaF and SiF_4. Using the different decomposition temperatures, separate recovery of HF and SiF_4 is achieved. The main reactions are as follows:

$$NaF{\cdot}nHF = NaF + nHF\uparrow \text{ (above 160 °C)} \quad \text{(R19)}$$

$$Na_2SiF_6 = NaF + SiF_4\uparrow \text{ (above 600 °C)} \quad \text{(R20)}$$

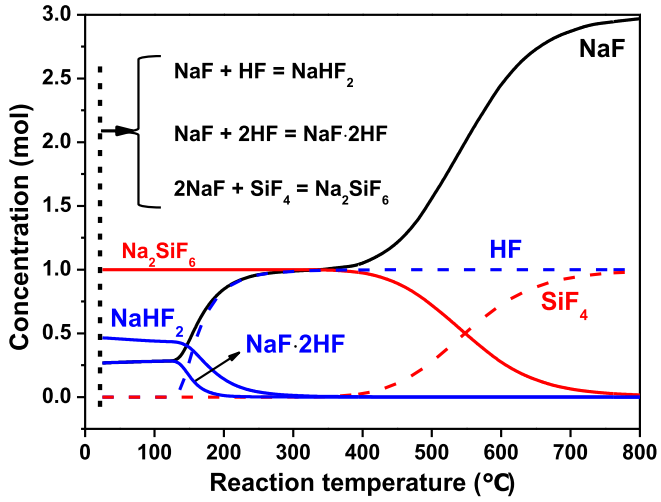

Fig. 11. Chemical equilibrium calculation for adsorption-desorption of fluoride and the molar ratio of NaF, HF and SiF_4 is 3: 1: 1.

Fig. 12 illustrates the XRD (X-ray diffraction) patterns of adsorbents placed at the top, middle and bottom of the reactor after adsorption of residual fluoride in the exhaust gas for 72 h. It can be seen that villiaumite adsorbents mainly consisting of NaF effectively absorbed HF and SiF_4 and converted them into $NaHF_2$ and Na_2SiF_6. NaF diffraction peaks were mainly found at 38.9° and 56.1°; the $NaHF_2$ peaks were at 32.4°, 44.6° and 52.7°; and the Na_2SiF_6 peaks were at 20.9°, 26.7° and 39.5°. The different peaks for each crystalline phase indicated that several crystalline planes were present, including (2 0 0) and (2 2 0) planes for NaF, (0 1 2), (0 1 5) and (1 1 0) planes for $NaHF_2$, and (1 0 1), (1 1 1) and (3 0 1) planes for Na_2SiF_6. The peak areas for each crystalline phase are usually related to their percentages (Arvelakis et al., 2006). As shown in Fig. 12, the peak area for NaF in the absorbent decreased from the top to the bottom of the reactor, while those of $NaHF_2$ and Na_2SiF_6 gradually increased, mainly because the lower absorbents preferentially reacted with HF and SiF_4 in the exhaust gas.

According to the sampling method introduced in Section 3.2.2, the concentration of fluoride in the exhaust gas was measured after it had passed through the defluorination device, and the results were 6.8, 12.4, and 8.2 mg/Nm^3, respectively, which met the requirement that the concentration of fluoride in the desulfurization process cannot exceed 30 mg/Nm^3. These results indicated that this method achieved high-efficiency defluorination and the efficiency could reach 91.5%.

3.3.2. Fluoride recycle

To further explore the regeneration of the adsorbents, 100 g of adsorbent was taken from the upper, middle and bottom parts of the reactor and put into the oven for 2 h to effect full decomposition and measure the efficiency for recovery of HF. Based on the reference intensity ratio (RIR) method (Hillier, 2000), the initial amount of HF adsorbed before decomposition was quantitatively analyzed with the XRD results obtained in Fig. 12. The RIR quantitative analysis for XRD is given by:

$$\frac{I_j}{I_s} = RIR_s^j \frac{W_j}{W_s}$$

where W denotes the weight fraction, I denotes the intensity, and the subscripts j and s indicate phase j and standard phases, respectively. For the corundum (Al_2O_3) standard phase, the reference intensity ratio (RIR) was determined according to the most intense corundum peak, I_{cor}, and the most intense peak from phase j, I_j, in a 1:1 mixture by weight. If NaF is selected as the standard, the formula used to calculate the concentrations of any phase j can be converted as follows:

$$W_j = W_{NaF} \frac{RIR_{cor}^{NaF}}{RIR_{cor}^j} \frac{I_j}{I_{NaF}}$$

The RIR values of NaF, $NaHF_2$ and Na_2SiF_6 are queried as 3.83, 2.4 and 0.87, respectively from the PDF standards. Considering the differences in diffraction peak widths for the crystalline phases in the adsorbents, the intensity ratios can be more accurately calculated by integral intensity (i.e., peak area) of single greatest peak than linear intensity (i.e., peak height). The I_j/I_{NaF} of $NaHF_2$ and Na_2SiF_6 can be calculated from the latest XRD patterns and shown in Table 6.

Overlapping peaks usually affect the accuracy of quantitative results of RIR method (Lin and Song, 2017), but in this case, diffraction peaks of each phase are basically non-overlapping and have accurate RIR values. Therefore, quantitative results close to reality can be obtained by the RIR method. As shown in Fig. 13, the weight fraction of NaF in the adsorbents (after 72 h adsorption) located in the top, middle and bottom, respectively were shown as 63.54%, 51.27% and 41.57%, respectively through comparing the peak intensity with the original adsorbent.

Table 6
Ratio of the integral intensity between the $NaHF_2$, Na_2SiF_6 and NaF.

Phase	Top	Middle	Bottom
$NaHF_2$	0.128	0.228	0.378
Na_2SiF_6	0.064	0.104	0.160

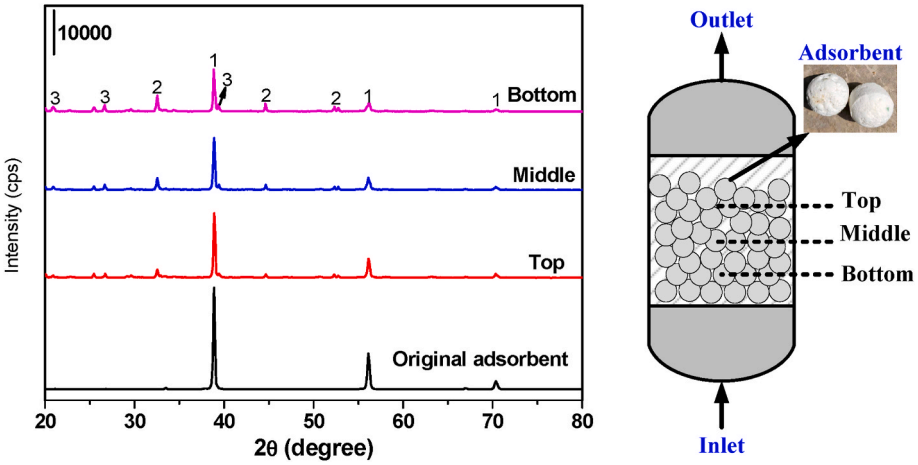

Fig. 12. XRD patterns after fluoride adsorption (72 h) for adsorbents placed at different locations in the reactor; the main crystalline phases can be identified as (1) sodium fluoride (NaF); (2) sodium bifluoride ($NaHF_2$); and (3) sodium fluosilicate (Na_2SiF_6).

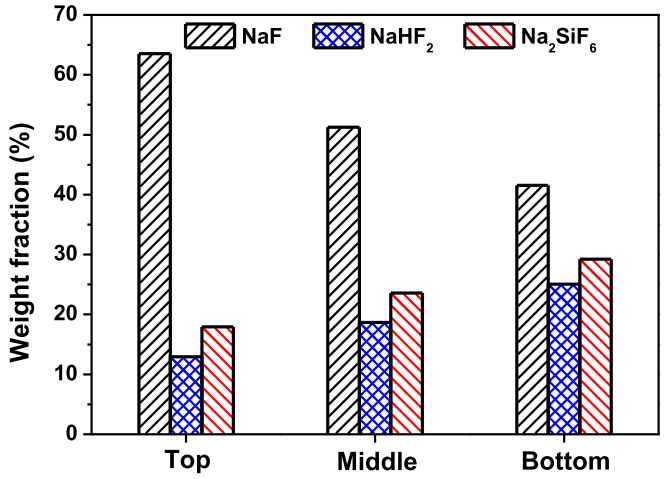

Fig. 13. Quantitative results for the main crystalline phases in the absorbent.

And then, the mass fractions of $NaHF_2$ in the adsorbents located at the top, middle and bottom of the reactor could be calculated as 12.94%, 18.66% and 25.06%, respectively, and that of Na_2SiF_6 were 17.93%, 23.56% and 29.24%, respectively. According to the calculated results, the mass fractions of HF in the adsorbents located at the top, middle and bottom of the reactor were 4.17%, 6.02% and 8.08%, respectively.

The released HF was absorbed by NaOH solution, and the total amount of HF was obtained by measuring the F^- content in the solution. The recovery efficiencies for HF were calculated from the ratio between the released amount and initial amount, and the results are shown in Table 7. This indicates that the adsorbents were regenerated effectively by heating, and the released HF can be directly condensed into anhydrous hydrofluoric acid or a certain concentration of hydrofluoric acid solution can be obtained by spraying. Considering that the decomposition temperature of Na_2SiF_6 is relatively high, the energy consumption is too large for practical applications, and SiF_4 gas is not easily recycled. Therefore, the adsorbents decomposed at 180 °C were put into the NaOH solution, and Na_2SiF_6 was converted into SiO_2 to realize the recovery of silicon species through the following reactions.

$$Na_2SiF_6 + 4NaOH \rightarrow 4NaF + 2SiO_2\downarrow + 2H_2O \quad \text{(R21)}$$

4. Discussion

Process comparison: There are essential differences between the dry process and wet spray process in terms of treatment of the exhaust gas produced by rare earth concentrates during roasting with concentrated sulfuric acid. The dry process not only involves simple replacement of equipment but also represents progress in the industrial production of rare earth elements. Compared with the original wet spray process, the dry processing technology, which mainly consists of a cyclone separator and heat exchangers, is simple, and less equipment is required; this reduces the initial investment in equipment by 50%. In addition, the dry process is more compact in terms of equipment layout, covering an area of approximately 55 m^2, while the equipment layout of the wet spray process requires at least 120 m^2. When the system is running, fewer personnel are required for operation of the dry process, which directly saves personnel costs for the plant. The maintenance points of the equipment are also decreased because of the smaller number of devices.

Comparison of power consumption: The electric equipment for the dry process mainly consists of a water circulating pump, make-up pump and acid pump, and the total power consumption is approximately 37 kW. At present, the electrical equipment used in the wet spray process includes a large number of spray circulating pumps and acid pumps, and the power consumption can reach 145.5 kW. In addition, equipment such as the filter presses used in wet process systems also consumes certain quantities of electricity. Therefore, compared with the original wet spray process, the new dry process considerably reduces electricity bills for the plant each year.

Comparison of natural gas consumption: At present, the concentration of mixed acid obtained by the wet spraying process is only 36%, and the separation of sulfuric acid and fluoric acid must be realized by the steaming acid process. And the concentration of sulfuric acid must be increased to more than 65% for reuse in the roasting process. The heat source for steaming the acid is the steam produced by natural gas used to support boiler combustion. Therefore, a large amount of natural gas is consumed to steam acid for the wet spraying process per year. However, the dry process designed in this article provides pure sulfuric acid with a concentration of approximately 77.6%, which can be directly used in the roasting process, and the concentration of mixed acid also exceeds 60%; this requires only a small amount of steam to obtain a specified concentration, which considerably reduces the amount of natural gas used in the plant. In addition, the dry process uses the heat of the exhaust gas to produce hot water for winter heating or produce steam for steaming acid through the steam drum, which further reduces energy consumption.

Comparison of water consumption: The cooling water needed for the dry process is all circulating water, and there is basically no water consumption. The only process that consumes water is conversion of water into steam. However, the original wet process requires water for spraying, which increases the consumption of water and produces a large amount of wastewater. As a result, the plant must also pay for wastewater treatment.

Table 7
Recovery rate of HF during the regeneration process of adsorbents.

Location	Initial amount (g)	Released amount (g)	Recovery rate (%)
Top	4.17	3.57	85.61
Middle	6.02	5.26	87.37
Bottom	8.08	6.95	86.01

5. Conclusion

In this paper, dry processing of the exhaust gas produced by rare earth concentrates during roasting with concentrated sulfuric acid is systematically introduced in an actual rare earth roasting kiln. Compared with the original wet spraying, the dry process greatly simplifies exhaust gas treatment and produces steam while achieving dust removal, cooling and acid condensation of the exhaust gas. During testing, slightly less than half of the total amount of exhaust gas entered the dry process system. The main conclusions are described below.

(1) Comparing with wet spraying, the dry process reduces the consume of water resource, realizes the utilization of waste heat from roasting exhaust gas and produces approximately 0.64 tons/h of steam through 1st heat exchanger and steam drum.
(2) The recovery efficiencies for sulfuric acid and fluoride reach 91.17% and 93.44%, respectively in the dry system, which is comparative with original wet system. However, the concentration of recycled sulfuric acid and mixed acid can reach to 77.6% and 63.58%, respectively, which is much higher than that of mixed acid produced by the wet spraying system with a mass fraction of only 36%. This will result in a significant reduction in energy consumption of acid steaming process.
(3) The dry defluorination process newly designed in the dry processing system further realizes the adsorption and recycle of residual fluoride (HF and SiF_4) through renewable adsorbents. The

efficiency for removal of fluoride reaches 91.5% and the average recovery efficiency of HF reaches 86.33%.

CRediT authorship contribution statement

Jing Zhao: Methodology, Software, Validation, Formal analysis, Investigation, Data curation, Writing – original draft, Visualization. **Bo Li:** Investigation, Conceptualization, Supervision, Methodology, Writing – review & editing. **Xiaolin Wei:** Conceptualization, Methodology, Supervision.

Declaration of competing interest

The authors declare that they have no known competing financial interests or personal relationships that could have appeared to influence the work reported in this paper.

Acknowledgements

This work is supported by the National Natural Science Foundation of China (No.51736010) and the Strategic Priority Research Program of the Chinese Academy of Sciences (No. XDA21040500). The authors also thank the plant for supplying some necessary data.

References

Arvelakis, S., Folkedahl, B., Dam-Johansen, K., Hurley, J., 2006. Studying the melting behavior of coal, biomass, and coal/biomass ash using viscosity and heated stage XRD data. Energy Fuel. 20, 1329–1340.

Asakai, T., Hioki, A., 2010. Investigation on drying conditions and assays of amidosulfuric acid and sodium carbonate by acidimetric coulometric titration and gravimetric titration. Accred Qual. Assur. 15, 391–399.

Bian, Z.T., Wang, X.F., Wang, C.Z., 2018. Research progress on rare tail gas treatment of rare earth concentrate. China Resour. Compr. Util. 36, 70–72 (in Chin.).

Chen, J.Y., Zhu, X.H., Liu, G., Chen, W.Q., Yang, D.H., 2018. China's rare earth dominance: the myths and the truths from an industrial ecology perspective. Resour. Conserv. Recycl. 132, 139–140.

Chen, J.L., Liu, L.Y., Dong, F.Z., Xie, J., Wang, Y.L., Jia, X.P., 2012. Addition of iron mud to Baotou mixed rare earth concentrate in its roasting decomposition with sulfuric acid. Chinese Rare Earth 33, 96–97 (in Chin.).

Chen, S.L., Huang, X.W., Feng, Z.Y., Xu, Y., Wang, M., Xia, C., Zhao, L.S., 2020. Behavior of rare earth, iron, and phosphorus during purification of rare earth sulfate leach solution using magnesium oxide. Hydrometallurgy 196, 105377.

Demol, J., Ho, E., Soldenhoff, K., Senanayake, G., 2019. The sulfuric acid bake and leach route for processing of rare earth ores and concentrates: a review. Hydrometallurgy 188, 123–139.

Demol, J., Ho, E., Senanayake, G., 2018. Sulfuric acid baking and leaching of rare elements, thorium and phosphate from a monazite concentrate: effect of bake temperature from 200 to 800°C. Hydrometallurgy 179, 254–267.

Gromov, O.B., 2014. System researches "fluorides of alkaline metals-hydrogen fluoride". Procedia Chem. 11, 30–34.

Han, J.K., Liu, X.W., Jiang, M., Wang, Z.F., Xu, M.H., 2021. A novel light scattering method with size analysis and correction for on-line measurement of particulate matter concentration. J. Hazard Mater. 401, 123721.

Hillier, S., 2000. Accurate quantitative analysis of clay and other minerals in sandstones by XRD: comparison of a Rietveld and a reference intensity ratio (RIR) method and the importance of sample preparation. Clay Miner. 35, 291–302.

Huang, X.W., Long, Z.Q., Wang, L.S., Feng, Z.Y., 2015. Technology development for rare earth cleaner hydrometallurgy in China. Rare Met. 34 (4), 215–222.

Jordens, A., Cheng, Y.P., Waters, K.E., 2013. A review of the beneficiation of rare earth element bearing minerals. Miner. Eng. 41, 97–114.

Kim, E., Osseo-Asare, K., 2012. Aqueous stability of thorium and rare earth metals in monazite hydrometallurgy: Eh-pH diagrams for the systems Th-, Ce-, La-, Nd-(PO_4)-(SO_4)-H_2O at 25°C. Hydrometallurgy 113–114, 67–68.

Li, B., Rong, X., Yao, Y., Wei, X.L., 2021. Research of resource utilization of high-temperature flue-gas of smelting furnace for rare earth concentrate. J. Therm. Sci. Technol. 20, 271–277 (in Chin.).

Li, J.F., Li, M., Zhang, D.L., Gao, K., Xu, W., Wang, H.H., Geng, J.L., Ma, X.F., Huang, L., 2019. Clean production technology of selective decomposition of Bayan Obo rare earth concentrate by NaOH. J. Clean. Prod. 236, 117616.

Lin, W.W., Song, Y.G., 2017. A comparative study on X-ray diffraction mineral quantitative analysis of two methods in sediments. J. Earth Environ. 8, 78–87 (in Chin.).

Nie, D.P., Zhang, Y., Xue, A., Zhu, M.Y., Cao, J.X., 2018. Migration behavior, separation and recycling of rare earth during thermal decomposition of Zhijin phosphorus ore. J. Rare Earths 36, 1205–1211.

Noh, S.Y., Heo, J.E., Woo, S.H., Kim, S.J., Ock, M.H., Kim, Y.J., Yook, S.J., 2018. Performance improvement of a cyclone separator using multiple subsidiary cyclones. Powder Technol. 338, 145–152.

Swain, N., Mishra, S., 2019. A review on the recovery and separation of rare earths and transition metals from secondary resources. J. Clean. Prod. 220, 884–898.

Singh, V.S., Moharil, S.V., 2020. Synthesis and study of luminescence in Na_2SiF_6. Mater. Today 28, 37–39.

Tavakoli, H., Ghasemi, M.R., 2010. Equilibrium, kinetics and breakthrough studies for adsorption of hydrogen fluoride on sodium fluoride. Chem. Eng. Process 49, 435–440.

Wang, L.S., Huang, X.W., Yu, Y., Zhao, L.S., Wang, C.M., Feng, Z.Y., Cui, D.L., Long, Z.Q., 2017. Towards cleaner production of rare earth elements from bastnaesite in China. J. Clean. Prod. 165, 231–242.

Wang, X.Y., Liu, J.M., Li, M., Fan, H.L., Yang, Q.S., 2010. Decomposition reaction kinetics of Baotou RE concentrate with concentrated sulfuric acid at low temperature. Rare Met. 29, 121–125.

Wang, Z.Q., Ma, Y.H., Deng, K.H., Liu, J., 2018. Exhaust gas treatment in rare earth roasting off-gas and comprehensive utilization of SO_2. Sulphuric Acid Ind. 11, 33–36 (in Chin.).

Xie, F., Zhang, T.A., Dreisinger, D., Doyle, F., 2014. A critical review on solvent extraction of rare earths from aqueous solutions. Miner. Eng. 56, 10–28.

Yang, D.L., Gao, S., Hong, J.L., Ye, L.P., Ma, X.T., Qi, C.C., Li, X.Z., 2019. Life cycle assessment of rare earths recovery from waste fluorescent powders-A case study in China. Waste Manag. 99, 60–70.

Zhang, L.P., Xing, Z., Feng, L., Li, H., 2007. Determination of standard value of sulfate standard solution by ion chromatography. Chin. J. Chromatogr. 25, 241–244 (in Chin.).

Zhao, M., Hu, Z.B., Pang, H., 2013. Research the tail gas treatment of Baotou rare earth concentrate by concentrated sulfuric acid roasting. Sci. Technol. Baotou Steel 39, 45–47 (in Chin.).

Zheng, Q., Wu, W.Y., Bian, X., 2017. Investigations on mineralogical characteristics of rare earth minerals in Bayan Obo tailings during the roasting process. J. Rare Earths 35, 300–308.

Zhong, B.Q., Wang, L.Q., Liang, T., Xing, B.S., 2017. Pollution level and inhalation exposure of ambient aerosol fluoride as affected by polymetallic rare earth mining and smelting in Baotou, north China. Atoms. Environ. 167, 40–48.

Zhou, L., Ge, J.P., 2021. Estimating the environmental cost of mixed rare earth production with willingness to pay: a case study in Baotou, China. Ext. Ind. Soc. 8, 340–354.